Rapid Communications

Evidence for a correlated phase of skyrmions observed in real space

John N. Moore,[1] Hikaru Iwata,[1] Junichiro Hayakawa,[1] Takaaki Mano,[2] Takeshi Noda,[2] Naokazu Shibata,[1] and Go Yusa[1,3,*]

[1]*Department of Physics, Tohoku University, Sendai 980-8578, Japan*

[2]*National Institute for Materials Science, Tsukuba, Ibaraki 305-0047, Japan*

[3]*Center for Spintronics Research Network, Tohoku University, Sendai 980-8578, Japan*

(Received 27 June 2018; revised manuscript received 29 August 2018; published 8 October 2018)

We conduct photoluminescence microscopy that is sensitive to both electron and nuclear spin polarization to investigate the changes that occur in the magnetic ordering in the vicinity of the first integer quantum Hall state in a GaAs two-dimensional electron system (2DES). We observe a discontinuity in the electron spin polarization and nuclear spin longitudinal relaxation time which heralds a spontaneous transition in the magnetic ordering. We image in real space the spin phase domains that coexist at this transition, and observe hysteresis in their formation as a function of the 2DES's chemical potential. Based on measurements in a tilted magnetic field orientation, we found that the transition is protected by an energy gap containing the Zeeman energy. We explain that these observations are consistent with a phase of skyrmions forming at the transition.

DOI: 10.1103/PhysRevB.98.161402

I. INTRODUCTION

A two-dimensional (2D) electron system (2DES) becomes strongly correlated at low temperatures when a strong magnetic field normal to it $B_\perp$ creates Landau levels (LLs) with energy separation large enough that many-body Coulomb interactions dominate the physics. The fractional quantum Hall (QH) effect, in which a gap in the density of states (DOS) is opened at fractional values of the LL filling factor ν, is one result of these correlations, as are the enhancement of screening, magnetization, and the transport activation gap at integer ν [1–6]. Particular interest has been given to the first integer QH state in GaAs, which is complicated beyond a single-particle picture by the presence of magnetic skyrmions [7]. Skyrmions are quasiparticles with a vortexlike spin texture resulting from competition between Zeeman and Coulomb interactions theorized to form when electrons are added to or removed from the ferromagnetic state at $\nu = 1$ [8]. Extensive evidence of skyrmions comes from observed reductions in electron polarization P and nuclear spin longitudinal relaxation time T_1, which are both consequences of the in-plane spin components of skyrmions [9–18]. However, there is only a very limited picture of how skyrmions form and interact.

Here we conduct detailed measurements of P and T_1 using spin-sensitive photoluminescence (PL) microscopy in an effort to study the critical conditions at which QH skyrmions form while visualizing their long-range behavior. An abrupt change in P and T_1, which occurs as the chemical potential of the 2DES traverses the neighborhood of $\nu = 1$, signals a discontinuous transition to what we interpret as a skyrmion-rich phase. The discontinuity of the transition is confirmed by real-space imaging of coexisting spin phase domains which exhibit hysteresis. We also show that the transition is protected by a gap in the DOS containing the Zeeman energy E_Z.

II. EXPERIMENT

Experiments were conducted in a dilution refrigerator on 2DESs in modulation-doped 15-nm GaAs quantum wells (QWs) etched into a Hall bar geometry. We present results from two devices (devices A and B [Figs. 1(a) and 1(b)]) differing in electron mobility by ∼50% [19]. The devices are equipped with a back gate allowing electron density n_e to be tuned by a gate voltage V_g and allowing us to create the first integer QH state over a wide range of $B_\perp$ (up to 10 T in device A) according to $\nu = hn_e/eB_\perp$, where h and e are the Planck constant and the elementary charge [20]. *However, the exact value of ν is not accessible experimentally because it depends on the details of the macroscopic DOS under the influence of disorder and interactions.* In the literature conventionally, n_e is approximated by CV_g/e, where C is a constant capacitance per unit area between the 2DES and the gate electrode. More exactly, though, C is not constant because the DOS has gaps, and strong electron interaction can cause the DOS to change unpredictably with small changes in V_g and B, particularly near $\nu = 1$. Therefore, n_e and ν are not suitable parameters to describe the narrow range of conditions examined here. Instead, we define a unitless chemical potential $\mu \equiv \frac{hC_0V_g/e}{eB_\perp} + \alpha$; here, C_0V_g/e is analogous to the change in n_e caused by V_g, where C_0 is defined as a constant capacitance per unit area of the gate, measured at total magnetic field $B \approx 0$; α is an offset which we define such that $\mu = 1$ at the center of the plateau in Hall resistance R_{xy}. Thus μ is comparable to the conventional estimate of ν in a gated 2DES.

Our method in these experiments was to collect σ^--polarized PL emitted from the QW, corresponding to recombination of electrons in the bottom Zeeman level (ZL), while illuminating the device with weak linearly polarized light of energy 1.579 eV. At the conditions of our experiment the PL has a spectrum containing up to two visible peaks which correspond to trions. Trions are bound states of two conduction band electrons with a valence band hole, and

*yusa@m.tohoku.ac.jp

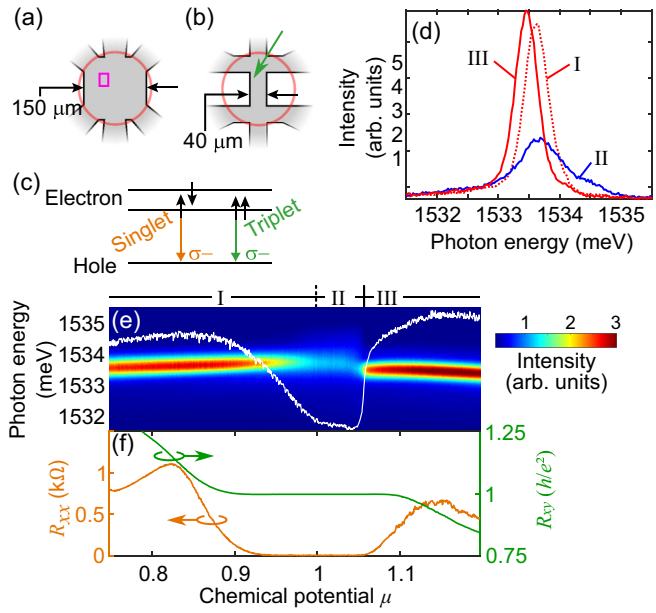

FIG. 1. Diagrams of Hall bars of (a) device A and (b) device B. Red circles: regions of illumination and macroscopic PL collection. Pink rectangle: region of PL spatial mapping. Green arrow: point of T_1 measurement ∼6 μm from edge. (c) Energy diagram of singlet and triplet trions and their optical transitions for photoluminescence. (d) PL spectra collected from regions I, II, and III, specifically $\mu = 0.86$, 1.03, and 1.1, respectively. (e) PL spectra as a function of μ measured macroscopically. White curve: integrated intensity of the trion singlet state PL peak ("PL intensity"). (f) Longitudinal resistance R_{xx} and Hall resistance R_{xy} vs μ. Throughout, unless otherwise specified, T is ∼45 mK, B is 8 T perpendicular to the 2DES; I_{sd} is 10 nA, 13 Hz.

they have a total electron spin of $S = 0$ or $S = 1$ depending on whether their electrons are in the singlet or triplet state [Fig. 1(c)] [21,22]. Theoretical treatment of the trions has indicated their usefulness in describing a 2DES in the QH state [23,24], and experimentally trions have been used to study the QH system at a variety of different conditions including the vicinity of $\nu = 1$ [18,25–27]. Here we use the intensity of the singlet trion peak to measure P as in previous work [28–30]. When an electron is photoexcited into the bottom ZL it forms a trion with an electron preexisting in the 2DES in the conduction band and the photoexcited hole. The probability that this trion is a singlet (triplet) trion is (anti-)correlated with the fraction of conduction electrons that are in the upper ZL. Consider that no singlet trions can form in the absence of spin-down electrons. Thus, the number of singlet trions that form by this process is anticorrelated to P. This number also has a linear relationship with the intensity of the σ^--polarized singlet trion PL, so by measuring this intensity we access a quantity that is anticorrelated to P.

III. RESULTS AND DISCUSSION

We first study how P changes in the QH liquid over the relatively wide range of $\mu = 1 \pm \sim 20\%$. Figure 1(e) shows σ^--polarized PL spectra collected from a 165-μm-diameter region (red circle) of the Hall bar in Fig. 1(a). PL spectra were measured simultaneously with transport [Fig. 1(f)] at B of 8 T and T of 45 mK while scanning μ by increasing V_g. The PL peak appearing in red originates from the singlet state, while the triplet state peak is dimly visible at 1534.5 meV near $\mu = 1$. After fitting the singlet peak to a Lorentz function, this peak's intensity, hereafter called "PL intensity," is integrated over a 390-μeV energy width and plotted as the white curve. Qualitatively we identify three regions of this curve, which we label as I, II, and III. Figure 1(d) shows representative spectra from each region. In region II, the PL intensity shows a broad minimum, indicating a broad maximum in P, which has been observed in other studies and measured to have a value of $P \approx 80\%$ [14–17,31]. P's reduction from 100% has been attributed to the existence of disorder-localized skyrmions and/or antiskyrmions [13–15]. It is still conceivable, though, that the 2DES becomes ferromagnetic in some microscopic regions. Experiments also conclude that in regions I and III where P is greatly diminished, antiskyrmions and skyrmions are present as a crystal or liquid phase [13,14,32,33]. We now observe that while the transition between regions I and II is gradual and continuous, the transition between regions II and III is abrupt.

We turn our attention to investigating the sharp transition in P at $B = 8$ T over the extremely narrow range $\mu = 1.057\,75 \pm 0.09\%$. Collecting PL from an ∼1-μm spot (μ-PL), we performed scanning microscopy of PL intensity where the feature occurs, and obtained the images in Figs. 2(a)– 2(d) taken inside the pink rectangle indicated in Fig. 1(a). We observed two distinct domains (blue and red) of differing PL intensity in Figs. 2(a) and 2(b) to collapse into a homogeneous state of high PL intensity in Fig. 2(d). The strong contrast between the PL spectra in the two domains is apparent in the spectra in Fig. 2(e) obtained at points 1 and 2 of Fig. 2(b). The evolution of these images is also captured in their histograms [Fig. 2(f)], in which two well-separated peaks corresponding to the two domains give way to a single peak. We conclude that we have witnessed this area of the sample undergo a transition between the macroscopically identified regions II and III, corresponding to the blue and red domains, respectively. We also find that whenever the two domains are both present, the autocorrelation coefficient for the images is larger than when $\mu \approx 2/5$ [19]. This indicates that there is a mechanism of ordering as strong as the the QW's disorder potential (∼100 μeV [28]) which is causing the domains to extend over several tens of micrometers.

In Fig. 3(a) we present μ-PL intensity as a function of μ taken at the five points (i–v) indicated in Fig. 2(d), which have 6-μm spacing. Hysteresis appears when scanning μ across the transition. The hysteresis at location v was reproducible, having a width of 0.0006 ± 0.0002 [19]. We conclude from this hysteresis that the transition separating regions II and III in Fig. 1(e) is first order.

We next seek to examine the magnetism of the 2DES from the perspective of T_1; T_1 is sensitive to the electronic spin ordering because hyperfine interaction with electrons is one mode of nuclear spin relaxation. Mismatch in electron and nuclear Zeeman energies normally makes this process very inefficient. However, in the presence of a gapless spin wave mode, the energy mismatch can be compensated while satisfying angular momentum conservation, and this leads to a

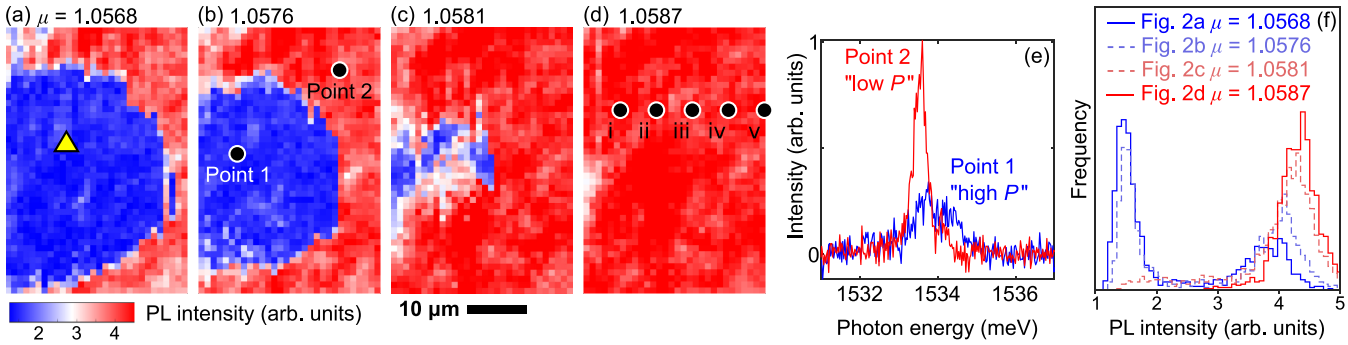

FIG. 2. (a)–(d) 33 × 40-μm^2 spatial images of the trion singlet state PL intensity at μ of (a) 1.0568, (b) 1.0576, (c) 1.0581, and (d) 1.0587. (e) Example PL spectra collected microscopically in the high-P region (blue) and low-P region (red) as part of the spatial mapping. (f) PL intensity histograms of the images.

significant reduction in T_1 [9]. In the QH system, such gapless spin waves require XY spin ordering because states that are collinear with B such as the QH ferromagnetic only support spin waves that are gapped by E_Z [9,34,35].

T_1 is experimentally accessible to us because the PL intensity is also sensitive to the degree of local nuclear polarization P_N by a mechanism we speculate is related to the Overhauser field's influence on the trions [30,36–38]. In the following experiment, we dynamically create P_N using the flip-flop scattering that occurs between electron and nuclear spins at the boundary of nonequilibrium stripe spin phase domains at $\nu \approx 2/3$ [29,30]. This allowed us to detect the decay of P_N in time by a procedure of repeatedly pumping the source-drain current I_{sd} to create P_N and then waiting a variable time before measuring the remaining P_N by the PL intensity [19]. T_1 changes depending on the μ at which we wait.

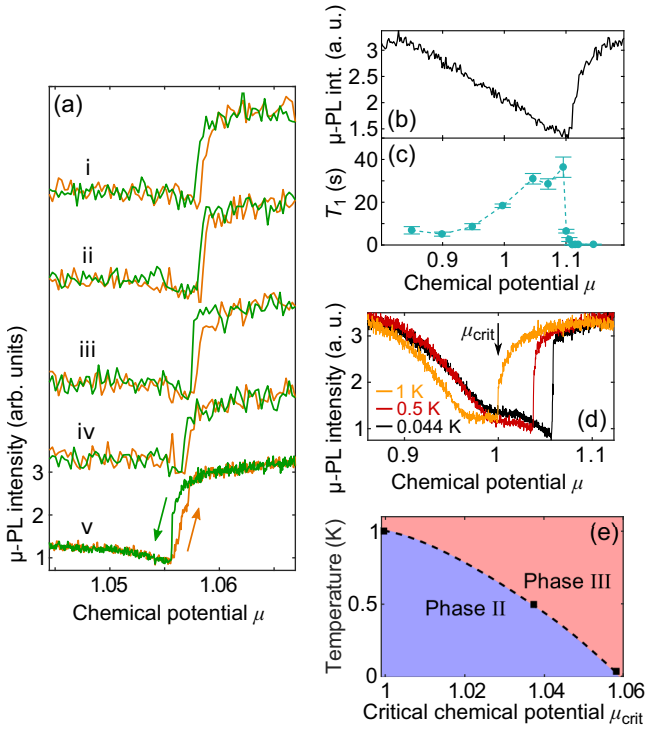

FIG. 3. (a) μ-PL intensity, offset for clarity, vs μ at locations i–v measured by forward and backward scans of μ with round-trip scan times of 10.6 min (i–iv) and 187.2 min (v). (b) μ-PL intensity and (c) T_1 measured microscopically vs μ. For (b) and (c), device B was used, and T was ~40 mK, $B = 6$ T. (d) μ-PL intensity vs μ at three temperatures. (e) Phase diagram in T vs μ_{crit}. Dashed line is a guide to the eye. Error estimates are discussed in the Supplemental Material [19].

In Figs. 3(b) and 3(c) we show μ-PL intensity and T_1 measured as a function of μ at the point in device B indicated by the green arrow in Fig. 1(b). Both of these data indicate a spontaneous change in spin ordering at roughly the same $\mu \approx 1.1$ corresponding to the first-order transition [39]. We define this critical μ as μ_{crit}. The relatively large T_1 value occurring just below μ_{crit} indicates a ferromagnetic or strongly polarized state, and the extremely short value of T_1 above μ_{crit} and around 0.9 in Fig. 3(c) is the expression of the gapless spin wave mode that is enabled by an in-plane component of electron spin ordering. Such a spin wave mode is created in the presence of skyrmions and antiskyrmions [9,40]. Another possibility is that a spin-frustrated Wigner crystal phase is responsible for creating the spin wave mode; however, there is currently little evidence for this form of magnetic ordering in the quantum Hall system.

We state here, and confirm below, that region II corresponds to the gap in the DOS between the ZLs of the lowest LL. This gap should contain both Zeeman and Coulomb components. Consider the following interpretation: ν becomes approximately 1 at the bottom of this gap, and then does not increase significantly until the top of the gap, which is why P has been observed to become plateaulike. At μ_{crit}, ν increases sharply as skyrmions form up to some critical density. The discontinuity in n_e across the transition might account for why the domain wall in Figs. 2(a) and 2(b) is concave with respect to phase II; the blue (red) region tends to expand (contract) in some places to maintain the low (high) density of phase II (the skyrmion phase).

To investigate the energy gap, we measured μ-PL intensity vs μ at three different temperatures [Fig. 3(d)] at the point indicated by the yellow triangle in Fig. 2(a). Increasing T from 44 mK to 1 K caused μ_{crit} to shift to lower μ, as is depicted in Fig. 3(e), and caused region II seen in the μ-PL intensity to shrink by ~50% [41]. A combination of factors may be causing region II to shrink. Thermal energy might be exciting ground electrons at the Fermi level into the upper ZL, which then triggers the phase transition to occur.

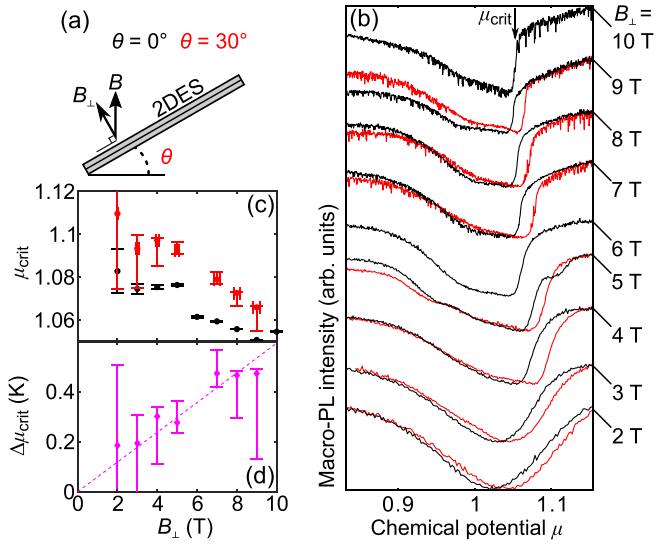

FIG. 4. (a) Schematic of the 2DES of device A tilted in the magnetic field. (b) Macroscopic PL intensity, normalized and offset for clarity, vs μ as a function of $B_\perp$ when $\theta = 0^\circ$ (black) and 30° (red). (c) $\mu_{\rm crit}$ vs $B_\perp$ for $\theta = 0^\circ$ (black) and 30° (red). (d) $\Delta\mu_{\rm crit}$ vs $B_\perp$. Dashed line: fitting function $mB_\perp$, where $m = 0.06 \pm 0.01$ K/T. Error estimates are discussed in the Supplemental Material [19].

Additionally, the gap energy may be reduced when thermal fluctuations disrupt the exchange correlations stabilizing the spin-polarized regions of phase II. As T increases, the change in μ-PL intensity at $\mu_{\rm crit}$ becomes diminished. This is possibly because when $\mu_{\rm crit}$ is less there is less chemical potential available for the creation of skyrmions, or possibly because skyrmions are reduced in size by thermal fluctuations. We do not present T_1 measured at elevated temperatures because above $\sim$100 mK the $P_{\rm N}$ needed for this measurement cannot be generated with the magnitude necessary. This is due to the thermal destabilization of the domains at $\nu \approx 2/3$.

The strong sensitivity of $\mu_{\rm crit}$ to T indicates that the gap energy is comparable to the thermal energy. We estimate the size of the gap's energy E_g by calculating how much thermal energy is required to shrink the width of region II to zero, and obtain $E_g = 1.9 \pm 0.4$ K, which we take to be E_g at the limit of 0 K [19]. This indicates that E_g can exceed E_Z, which is $\sim$1.7 K at 8 T. Such an outcome is expected in order for E_g to be equal to either the Zeeman plus exchange energy cost of a single spin flip, or the cost of a skyrmion; the latter energy cost contains a large Zeeman component, but can have a net negative Coulomb component due to quantum fluctuations afforded by the superpositional states of the skyrmion's spins [42].

We now probe the energy gap further by returning to measurements of PL intensity from the circular macroscopic region in Fig. 1(a). In order to isolate the contribution of Zeeman energy to the gap, we also tilt the device with respect to B in the configuration of Fig. 4(a) while holding $B_\perp$ fixed. This increases E_Z while leaving the orbital dynamics unchanged [43]. As such, the ratio between Zeeman and Coulomb energy $\eta = E_Z/E_C$ increases by $\sim$20% upon tilting the device in this experiment [44]. Figure 4(b) shows PL

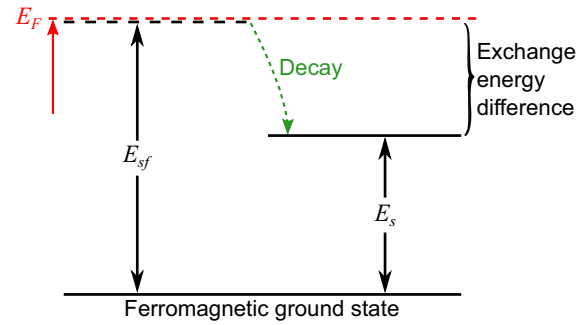

FIG. 5. Energy diagram of the ferromagnetic ground state and excited quasiparticle states as the Fermi energy is raised above the single-spin-flip quasiparticle excitation energy E_{sf}. E_s: skyrmion excitation energy.

intensity at tilt angles θ of 0° (black) and 30° (red) as a function of μ over a range of $B_\perp$. $\mu_{\rm crit}$ is plotted in Fig. 4(c) against $B_\perp$ for both conditions of θ. When tilting the sample 30°, the transition remains sharp, and $\mu_{\rm crit}$ increases while region II tends to become wider. This indicates that the gap protecting the phase transition has been expanded by the increase in E_Z. To measure the gap's expansion, we convert the difference in $\mu_{\rm crit}$ between the two tilt angles $\Delta\mu_{\rm crit}$ to units of kelvin [19]. $\Delta\mu_{\rm crit}$, plotted in Fig. 4(d), tends to scale with B, which confirms that it is proportional to E_Z; thus E_g is linear with E_Z.

As $B_\perp$ grows, η increases from 0.0053 at 2 T to 0.0119 at 10 T in the untilted case, and the PL intensity change vs μ (or V_g) at the transition becomes sharper. The high field and low temperature required for the transition to manifest sharply partly accounts for why the asymmetry in P and T_1 have not been clearly observed in some other studies. Note that the asymmetry manifests clearly in Ref. [13]. If region III contains a phase of skyrmions, the sharpness of the transition implies that upon creation of the first skyrmion, it takes very little additional chemical potential to create additional skyrmions up to a critical density. The additional chemical potential cost even would seem to be negative because, as observed, the skyrmion phase spontaneously overcomes the background potential. This is not intuitive, though, because skyrmions repel each other through short-range magnetic and long-range electrostatic interactions [40].

Nonetheless, the spin texture that forms at the phase transition may be made up of skyrmions if the following speculation based on the diagram in Fig. 5 is correct. Consider the fact that adding or subtracting a skyrmion requires spin reorientations involving exchange of angular momentum between several electrons and the environment, and this process cannot occur as a single quantum transition. Only after the Fermi energy E_F becomes high enough to add a single spin-flipped electron into the spin-polarized 2DES, a skyrmion can begin to form with this electron as its nucleus. After the skyrmion finishes forming, the electrons have decayed into a ground state at an energy lower than E_F. E_F is thus high enough to add another spin-flipped electron to the 2DES, perpetuating a chain reaction that nucleates additional skyrmions. The reverse of this process occurs when E_F falls below the skyrmion ground-state energy. This causes skyrmions to be

destroyed in an irreversible process in which the electron at the skyrmion nucleus is removed from the 2DES and the surrounding electrons relax into a ferromagnetic configuration. In this view, the hysteresis of the transition derives from the difference between the single-spin-flip quasiparticle and skyrmion ground-state energies.

In conclusion, here, the lowest-energy stable excitation above $\nu = 1$ is not an individual skyrmion. Rather, it is a correlated spin texture which possibly contains an ensemble of many skyrmions.

ACKNOWLEDGMENTS

This work was supported by a Grant-in-Aid for Scientific Research (Grant No. 17H01037) from the Ministry of Education, Culture, Sports, Science, and Technology (MEXT), Japan and the Asahi Glass Foundation. J.N.M. was supported by a Grant-in-Aid from JSPS, MEXT, and the Marubun Research Promotion Foundation. J.H. was supported by a Grant-in-Aid from the Tohoku University International Advanced Research and Education Organization.

[1] J. P. Eisenstein and H. L. Stormer, Science **248**, 1510 (1990).

[2] N. Pascher, C. Rössler, T. Ihn, K. Ensslin, C. Reichl, and W. Wegscheider, Phys. Rev. X **4**, 011014 (2014).

[3] I. Meinel, D. Grundler, D. Heitmann, A. Manolescu, V. Gudmundsson, W. Wegscheider, and M. Bichler, Phys. Rev. B **64**, 121306(R) (2001).

[4] R. J. Nicholas, R. J. Haug, K. V. Klitzing, and G. Weimann, Phys. Rev. B **37**, 1294 (1988).

[5] A. Usher, R. J. Nicholas, J. J. Harris, and C. T. Foxon, Phys. Rev. B **41**, 1129 (1990).

[6] A. Schmeller, J. P. Eisenstein, L. N. Pfeiffer, and K. W. West, Phys. Rev. Lett. **75**, 4290 (1995).

[7] S. E. Barrett, G. Dabbagh, L. N. Pfeiffer, K. W. West, and R. Tycko, Phys. Rev. Lett. **74**, 5112 (1995).

[8] S. L. Sondhi, A. Karlhede, S. A. Kivelson, and E. H. Rezayi, Phys. Rev. B **47**, 16419 (1993).

[9] R. Côté, A. H. MacDonald, L. Brey, H. A. Fertig, S. M. Girvin, and H. T. C. Stoof, Phys. Rev. Lett. **78**, 4825 (1997).

[10] B. A. Piot, W. Desrat, D. K. Maude, D. Kazazis, A. Cavanna, and U. Gennser, Phys. Rev. Lett. **116**, 106801 (2016).

[11] K. Hashimoto, K. Muraki, T. Saku, and Y. Hirayama, Phys. Rev. Lett. **88**, 176601 (2002).

[12] S. Melinte, N. Freytag, M. Horvatic, C. Berthier, L. P. Levy, V. Bayot, and M. Shayegan, Phys. Rev. B **64**, 085327 (2001).

[13] T. Guan, B. Friess, Y. Li, S. Yan, V. Umansky, K. V. Klitzing, and J. H. Smet, Chin. Phys. B **24**, 067302 (2015).

[14] P. Khandelwal, A. E. Dementyev, N. N. Kuzma, S. E. Barrett, L. N. Pfeiffer, and K. W. West, Phys. Rev. Lett. **86**, 5353 (2001).

[15] V. Zhitomirsky, R. Chughtai, R. J. Nicholas, and M. Henini, Semicond. Sci. Technol. **19**, 252 (2004).

[16] P. Plochocka, J. M. Schneider, D. K. Maude, M. Potemski, M. Rappaport, V. Umansky, I. Bar-Joseph, J. G. Groshaus, Y. Gallais, and A. Pinczuk, Phys. Rev. Lett. **102**, 126806 (2009).

[17] E. H. Aifer, B. B. Goldberg, and D. A. Broido, Phys. Rev. Lett. **76**, 680 (1996).

[18] J. G. Groshaus, V. Umansky, H. Shtrikman, Y. Levinson, and I. Bar-Joseph, Phys. Rev. Lett. **93**, 096802 (2004).

[19] See Supplemental Material at http://link.aps.org/supplemental/10.1103/PhysRevB.98.161402 for (i) experimental details, (ii) disorder potential mapping, (iii) PL intensity and mapping at elevated T, (iv) reproducibility of hysteresis, and (v) data error and calculations of the DOS energy gap and E_Z, including Refs. [45–48].

[20] n_e is taken to be the average electron density over the area of the Hall bar. The local electron density at any given point is in general different from n_e.

[21] A. J. Shields, M. Pepper, M. Y. Simmons, and D. A. Ritchie, Phys. Rev. B **52**, 7841 (1995).

[22] G. Finkelstein, H. Shtrikman, and I. Bar-Joseph, Phys. Rev. B **53**, R1709 (1996).

[23] A. Wojs, J. J. Quinn, and P. Hawrylak, Phys. Rev. B **62**, 4630 (2000)

[24] J. J. Palacios, D. Yoshioka, and A. H. MacDonald, Phys. Rev. B **54**, R2296 (1996).

[25] G. Yusa, H. Shtrikman, and I. Bar-Joseph, Phys. Rev. Lett. **87**, 216402 (2001).

[26] I. Bar-Joseph, G. Yusa, and H. Shtrikman, Solid State Commun. **127**, 765 (2003).

[27] S. Nomura, M. Yamaguchi, H. Tamura, T. Akazaki, Y. Hirayama, M. Korkusinski, and P. Hawrylak, Phys. Rev. B **89**, 115317 (2014).

[28] J. Hayakawa, K. Muraki, and G. Yusa, Nat. Nanotechnol. **8**, 31 (2013).

[29] J. N. Moore, J. Hayakawa, T. Mano, T. Noda, and G. Yusa, Phys. Rev. B **94**, 201408(R) (2016).

[30] J. N. Moore, J. Hayakawa, T. Mano, T. Noda, and G. Yusa, Phys. Rev. Lett. **118**, 076802 (2017).

[31] L. Tiemann, G. Gamez, N. Kumada, and K. Muraki, Science **335**, 828 (2012).

[32] V. Bayot, E. Grivei, S. Melinte, M. B. Santos, and M. Shayegan, Phys. Rev. Lett. **76**, 4584 (1996).

[33] Y. Gallais, J. Yan, A. Pinczuk, L. N. Pfeiffer, and K. W. West, Phys. Rev. Lett. **100**, 086806 (2008).

[34] Y. A. Bychkov, S. V. Iordanskii, and G. M. Eliashberg, Pis'ma Zh. Eksp. Teor. Fiz. **33**, 152 (1981) [JETP Lett. **33**, 143 (1981)].

[35] C. Kallin and B. I. Halperin, Phys. Rev. B **30**, 5655 (1984).

[36] A. Abragam, *The Principles of Nuclear Magnetism* (Clarendon Press, Oxford, 1961), pp. 200.

[37] W. A. Coish and J. Baugh, Phys. Status Solidi B **246**, 2203 (2009).

[38] P_N can be ruled out as the cause of any of the phenomena so far discussed because the measurements do not employ high currents or intense circularly polarized illumination needed to dynamically generate P_N.

[39] The jump in T_1 occurs at ~0.02 lower μ than the jump in PL intensity. This is likely because at a location near to the measurement point the transition occurs at a lower μ, and nuclear spin diffusion into that location enhances the effective relaxation rate.

[40] C. Timm, S. M. Girvin, and H. A. Fertig, Phys. Rev. B **58**, 10634 (1998).

[41] In the macro-PL intensity as well, we observe all of the same general changes with T as seen microscopically.

[42] H. A. Fertig, L. Brey, R. Côté, and A. H. MacDonald, Phys. Rev. B **50**, 11018 (1994).

[43] F. F. Fang and P. J. Stiles, Phys. Rev. **174**, 823 (1968).

[44] Here $E_C = e^2/(4\pi\epsilon_0\epsilon_r\ell_B)$, where $\ell_B = \sqrt{\hbar/eB_\perp}$ is the magnetic length, and we take ϵ_r to be 12.15. $E_Z = |g^*|\mu_B B$, where the effective g factor g^* is a tensor with $|g^*_\perp| = 0.30$ and $|g^*_\parallel| = 0.36$ based on the measurements of W. Shichi, T. Ito, M. Ichida, H. Gotoh, H. Kamada, and H. Ando, Jpn. J. Appl. Phys. **48**, 063002 (2009); T. Ito, W. Shichi, Y. Nishioka, M. Ichida, H. Gotoh, H. Kamada, and H. Ando, J. Luminesc. **128**, 865 (2008); A. Malinowski and R. T. Harley, Phys. Rev. B **62**, 2051 (2000); I. A. Yugova, A. Greilich, D. R. Yakovlev, A. A. Kiselev, M. Bayer, V. V. Petrov, Yu. K. Dolgikh, D. Reuter, and A. D. Wieck, *ibid.* **75**, 245302 (2007).

[45] K. Akiba, S. Kanasugi, T. Yuge, K. Nagase, and Y. Hirayama, Phys. Rev. Lett. **115**, 026804 (2015).

[46] A. Wójs, A. Gładysiewicz, and J. J. Quinn, Phys. Rev. B **73**, 235338 (2006).

[47] C. Schüller, K.-B. Broocks, P. Schröter, Ch. Heyn, D. Heitmann, M. Bichler, W. Wegscheider, T. Chakraborty, and V. M. Apalkov, Phys. Rev. Lett. **91**, 116403 (2003).

[48] J. H. Davies, *The Physics of Low-dimensional Semiconductors* (Cambridge University Press, Cambridge, 1998) pp. 223–227; 392–393.